Inhibition of Cyclooxygenase-2 Suppresses Lymph Node Metastasis via Reduction of Lymphangiogenesis

Caname Iwata,[1,2] Mitsunobu R. Kano,[1,3] Akiyoshi Komuro,[1] Masako Oka,[1] Kunihiko Kiyono,[1] Erik Johansson,[1] Yasuyuki Morishita,[1] Masakazu Yashiro,[4] Kosei Hirakawa,[4] Michio Kaminishi,[2] and Kohei Miyazono[1,3]

Departments of [1]Molecular Pathology and [2]Gastrointestinal Surgery, Graduate School of Medicine, [3]Center for NanoBio Integration, University of Tokyo, Tokyo, Japan and [4]Department of Surgical Oncology, Medical School, Osaka City University, Osaka, Japan

Abstract

Cyclooxygenase-2 (COX-2) inhibitor has been reported to suppress tumor progression. However, it is unclear whether this inhibitor can also prevent lymphatic metastasis. To determine the effects of COX-2 inhibitor on lymphatic metastasis, etodolac, a COX-2 inhibitor, was given p.o. to mice bearing orthotopic xenografts or with carcinomatous peritonitis induced with a highly metastatic human diffuse-type gastric carcinoma cell line, OCUM-2MLN. Tumor lymphangiogenesis was significantly decreased in etodolac-treated mice compared with control mice. Consistent with this decrease in lymphangiogenesis, the total weight of metastatic lymph nodes was less in etodolac-treated mice than in control mice. Immunohistochemical analysis revealed that the major source of vascular endothelial growth factor-C (VEGF-C) and VEGF-D was F4/80-positive macrophages in our models. The mRNA levels of VEGF-C in mouse macrophage-like RAW264.7 cells, as well as those in tumor tissues, were suppressed by etodolac. The growth of human dermal lymphatic microvascular endothelial cells was also suppressed by etodolac. Supporting these findings, etodolac also inhibited lymphangiogenesis in a model of chronic aseptic peritonitis, suggesting that COX-2 can enhance lymphangiogenesis in the absence of cancer cells. Our findings suggest that COX-2 inhibitor may be useful for prophylaxis of lymph node metastasis by reducing macrophage-mediated tumor lymphangiogenesis. [Cancer Res 2007;67(21):10181–9]

Introduction

Lymph node metastasis is a common occurrence in cancer, and lymphatic vessels serve as an important route for the spread of cancer cells (1, 2). Lymphatic metastasis was previously believed to be a passive process in which detached cancer cells reach lymph nodes through preexisting local lymphatic vessels (3). However, recent studies have suggested that lymphangiogenesis actively contributes to metastasis based on the observations that lymphatic vessel density is correlated with the extent of lymph node metastasis and/or unfavorable prognosis of certain cancers (2, 4, 5). Moreover, some animal tumor models have revealed that

expression of lymphangiogenic growth factors leads to formation of lymphatic vessels and that lymphangiogenesis is accompanied by enhanced lymphatic metastasis (2). These findings strongly suggest that lymphatic metastasis can be blocked by inhibition of tumor lymphangiogenesis (1, 6, 7).

The best studied lymphangiogenic signaling system is the vascular endothelial growth factor-C (VEGF-C)/VEGF-D and VEGF receptor 3 (VEGF-R3) signaling axis, which has been shown to play a central role in lymphangiogenesis in animal models (1, 2, 4). Elevated expression of VEGF-C or VEGF-D has been observed in many human cancers (2, 4). A number of studies have shown that levels of expression of VEGF-C in primary tumor correlate with lymphatic vessel invasion and/or lymph node metastasis (2, 4, 8), although the correlation between VEGF-D and metastasis is currently unclear (4, 9). These ligands are thought to be secreted from tumor cells; in addition, macrophages in the peritumoral stroma (i.e., tumor-associated macrophages) have also been reported to produce VEGF-C and VEGF-D in certain cancers and to induce lymphangiogenesis (10). The contribution of inflammatory cells to lymphangiogenesis has also been shown in mouse models of inflammation (11, 12).

Epidemiologic studies have shown that regular intake of nonsteroidal antiinflammatory drugs (NSAID), prototypic inhibitors of cyclooxygenase (COX), such as aspirin, can reduce the risk of development of some cancers (13). In addition, overexpression of COX-2, which is induced by both inflammatory and mitogenic stimuli, is commonly found in many cancers (14–16), suggesting that COX-2 contributes to the process of carcinogenesis. Direct molecular evidence that *COX-2* contributes to carcinogenesis has been obtained from studies in animals engineered to be deficient in expression of the COX-2 gene (17) or treated with COX-2 selective inhibitors (18). Thus far, several mechanisms by which COX-2 contributes to progression of cancer have been reported, including stimulation of proliferation and inhibition of apoptosis of cancer cells, stimulation of cancer cell invasion and angiogenesis, and suppression of immune responses (14, 19).

The major role of COX-2 in angiogenesis is thought to be induction of the synthesis of prostanoids, which then stimulate the secretion of proangiogenic factors, including VEGF-A and fibroblast growth factor-2, from cancer cells and/or stromal fibroblasts (20, 21). In addition, COX-2 stimulates the proliferation (22), migration, and tube formation of vascular endothelial cells (20). Several clinical studies have indeed shown a correlation between level of COX-2 expression and extent of angiogenesis in cancer (23).

In contrast to the effect of COX-2 on angiogenesis, that on lymphangiogenesis remains poorly understood, although correlations between COX-2 expression and lymphangiogenesis or lymph node metastasis have been reported for several human cancers

(24–28). To examine whether COX-2 is involved in lymphatic metastasis, we evaluated the effects of treatment with a COX-2 selective inhibitor, etodolac (29, 30), on tumor lymphangiogenesis and extent of lymph node metastasis using a highly metastatic human diffuse-type gastric carcinoma cell line, OCUM-2MLN (31). We also examined the effects of etodolac on lymphangiogenesis in two other animal models, i.e., a model of carcinomatous peritonitis and one of chronic aseptic peritonitis. Our findings suggest that etodolac has antilymphangiogenic activity *in vivo* and that inhibition of COX-2 could suppress tumor lymphangiogenesis and lymph node metastasis.

Materials and Methods

Animals and cells. Immunodeficient BALB/c nu/nu mice at 4 to 5 weeks of age, obtained from Charles River Laboratories, were used for the model of lymph node metastasis and a model of carcinomatous peritonitis. Specific pathogen-free BALB/c mice at 4 to 5 weeks of age, obtained from Sankyo Laboratory, were used for a model of chronic aseptic peritonitis. Mice were treated in accordance with the policies of the Animal Ethics Committee of the University of Tokyo. OCUM-2MLN, a human diffuse-type gastric carcinoma cell line with a high rate of metastasis to lymph nodes, was previously established (31). RAW264.7, a mouse macrophage-like cell line, was a kind gift from Dr. Tadashi Muroi (NIH Sciences). Human dermal lymphatic microvascular endothelial cells (HDLEC) were obtained from Cambrex.

Model of lymph node metastasis. We used a lentiviral vector (a kind gift from Dr. Hiroyuki Miyoshi, RIKEN; ref. 32) to express the *green fluorescent protein* (*GFP*) gene stably in OCUM-2MLN. A total of 5×10^6 cells in 50 μL of PBS were subserosally inoculated into the gastric walls of BALB/c nu/nu mice as previously described (31) under deep inhalation anesthesia with ether. Four weeks after inoculation, the mice were sacrificed for evaluation. Etodolac (500 ppm in food; obtained from Nippon Shinyaku) or vehicle control was given p.o. throughout the experimental period from the inoculation of cancer cells until evaluation ($n = 7$ mice for each group). The experiment was repeated thrice.

Spread of cancer cells from the site of inoculation in the stomach was observed with a VB-G25 fluorescence stereomicroscope (Keyence). The captured fluorescence images and bright-field images were merged using Adobe Photoshop software (Adobe Systems). All GFP-positive, i.e., metastatic, lymph nodes were collected, and the total weight of these lymph nodes was measured. Stomachs were excised, fixed for 1 h in 10% neutral buffered formalin at room temperature, washed overnight in PBS containing 10% sucrose at 4°C, embedded in optimal cutting temperature compound (Tissue-Tek, Sakura Finetek), and snapped frozen in dry-iced acetone for immunohistochemical examination.

To visualize the lymphatic vessels in normal gastric wall, we injected India ink into the gastric wall of anesthetized control mice and immediately observed the draining lymphatic vessels by stereomicroscope.

Model of carcinomatous peritonitis. We i.p. injected OCUM-2MLN cells (5×10^6) into BALB/c nu/nu mice to induce carcinomatous peritonitis. The mice were sacrificed 2 weeks after inoculation and were evaluated. Etodolac (500 ppm in food) or vehicle control was given p.o. throughout the experimental period from injection of cancer cells until evaluation ($n = 5$ for each group). Diaphragms with disseminated tumor cells were excised, carefully extended, fixed for 30 min in 10% neutral buffered formalin at room temperature, and washed overnight in PBS containing 10% sucrose at 4°C. These diaphragms were embedded in optimal cutting temperature compound and snapped frozen in dry-iced acetone for immunohistochemical study or whole-mount immunostained. The experiment was repeated twice.

To visualize the lymphatic vessels in normal diaphragm, we i.p. injected India ink to control mice and observed the lymphatic vessels filled with ink in the diaphragms 20 min later.

Model of chronic aseptic peritonitis. We i.p. injected 2 mL of 3% thioglycollate medium (BBL thioglycollate medium, BD Biosciences) into

BALB/c mice thrice a week for 2 weeks to induce peritonitis. Etodolac (500 ppm in food) or vehicle control was given p.o. during the same period ($n = 5$ for each group). The mice were then sacrificed, and their diaphragms excised and prepared for H&E staining and immunostaining as described above. The experiment was repeated twice.

Immunohistochemistry. Whole mounts of diaphragms and 20-μm cryostat sections of postfixed frozen samples were stained with one or more primary antibodies. We used the following antibodies for immunostaining. For staining of lymphatic vessels, rabbit polyclonal antibody to LYVE-1 (1:200 dilution; Abcam), rat monoclonal antibody to mouse LYVE-1 (1:100 dilution; a kind gift from Drs. Yuichi Oike and Toshio Suda, Keio University), or rabbit polyclonal antibody to Prox1 (1:200 dilution; Chemicon) was used. Rat monoclonal antibody to mouse platelet/endothelial cell adhesion molecule 1 (PECAM-1; 1:200 dilution; BD PharMingen) was used for staining of blood vessels. For staining of VEGF-C and VEGF-D, goat polyclonal antibody to VEGF-C (C-20; 1:50 dilution, Santa Cruz Technology), and rabbit polyclonal antibody to VEGF-D (H-144; 1:50 dilution, Santa Cruz Technology) were used, respectively. Macrophages were immunostained with rat monoclonal antibody to F4/80 (1:20 dilution; Serotec) or rat monoclonal antibody to mouse CD11b (1:200 dilution; Chemicon). Dividing cells were stained with rabbit polyclonal antibody to Ki-67 (1:1,000 dilution; Novo Castra). COX-2 was stained with affinity-purified rabbit polyclonal antibody to COX-2 (1:100 dilution; Cayman Chemical). Subsequently, specimens were incubated with corresponding secondary antibodies labeled with Alexa Fluors 488, 594, or 647 (Invitrogen-Molecular Probes) at 1:200 dilution. Cell nuclei were counterstained with 20 μmol/L TOTO-3 (Invitrogen-Molecular Probes). In control experiments, the primary antibody was omitted. Specimens were examined with a LSM 510 META confocal microscope (Carl Zeiss) or a fluorescence stereomicroscope.

Morphometric analysis. In the model of lymph node metastasis, we double-stained tumor sections for LYVE-1 and PECAM-1 to examine lymphatic and blood vessel densities. For each tumor section, five hotspots (i.e., fields with the highest vascular density) in tumor areas were evaluated at magnification of 200×. Digital images of LYVE-1–positive lymphatic vessels and highly PECAM-1–positive blood vessels were captured. Area densities (percentage of total tissue area) of lymphatic vessels or blood vessels were then calculated using ImageJ software (NIH).

In the model of carcinomatous peritonitis, whole-mount diaphragms stained for LYVE-1 were evaluated from the pleural side. Lymphatic sprouts, defined as tapered projections, were counted at magnification of 100× in 10 microscopic fields per diaphragm.

In the model of chronic aseptic peritonitis, whole-mount diaphragms stained for LYVE-1 and CD11b were evaluated from the peritoneal side. Inflammatory plaques, defined as accumulations of inflammatory cells, especially of macrophages, had formed on the peritoneal surface of the diaphragm. For each diaphragm, 10 microscopic fields in inflammatory plaques were evaluated at magnification of 200×. Digital images of LYVE-1–positive lymphatic vessels were captured, and the area density of lymphatic vessel was calculated using ImageJ software.

RNA isolation and quantitative reverse transcription–PCR. Gastric walls with or without tumor were excised from mice, immersed in RNAlater (Qiagen), embedded in optimal cutting temperature compound, and snapped frozen. Total RNAs were extracted from tissue sections using the RNeasy micro kit (Qiagen). Total RNAs from RAW264.7 and HDLECs were extracted using the RNeasy mini kit (Qiagen). First-strand cDNAs were synthesized using the Quantitect reverse transcription kit (Qiagen) with random hexamer primers. Quantitative real-time reverse transcription–PCR (RT-PCR) analysis was done using the 7500 Fast Real-Time PCR system (Applied Biosystems). The primer sequences used are given in Supplementary Table S1.

Cell growth assay. Cell growth was determined with a WST-8 assay kit (Nacalai Tesque). Briefly, HDLECs (1×10^3 cells per well) or OCUM-2MLN (7.5×10^2 cells per well) in 96-well plates were incubated overnight. Thereafter, the medium was replaced with a new medium containing etodolac and/or lipopolysaccharide (LPS; O111:B4; Sigma-Aldrich). After 24 to 96 h of incubation, the WST-8 reagent was added to the culture. After

2 h of incubation, absorbance at 450 nm was measured with a microplate reader (Bio-Rad).

Statistical analysis. Statistical analysis was carried out using Excel software (Microsoft). Results were compared by Student's *t* test and expressed as mean values with SE. Differences were considered statistically significant at $P < 0.05$. All statistical tests were two-sided. Effects of etodolac on the growth of OCUM-2MLN were evaluated by multivariate ANOVA testing using JMP software (SAS Institute).

Results

Spread of cancer cells via lymphatic vessels in a murine model of lymph node metastasis of gastric cancer. To determine lymph node metastasis *in vivo*, we used an animal model of human metastatic gastric carcinoma, in which OCUM-2MLN cells expressing GFP were inoculated orthotopically into the gastric wall of BALB/c nu/nu mice. Examination by fluorescence stereomicroscope 4 weeks after inoculation revealed that the cancer cells had metastasized from the site of inoculation into the regional lymph nodes. Using this model, we examined tumor

lymphangiogenesis and spread of cancer cells through the lymphatic vessels. The cancer cells in this model exhibited invasion into peritumoral lymphatic vessels and spread along lymphatic vessels in the gastric wall toward the regional lymph nodes (Fig. 1*A*). Visualization by intravital injection of India ink into the gastric wall of control mice (Supplementary Fig. S1) revealed that the sizes and numbers of the lymphatic vessels were dramatically increased in the mice inoculated with gastric cancer cells (Fig. 1*A*) compared with those in control mice. To confirm the increase in lymphatic vessels in the mice bearing cancer cells, we double-stained the sections of the gastric wall of the mice using LYVE-1, a specific lymphatic vessel marker, and Ki-67, a marker of cell proliferation. Some dividing lymphatic endothelial cells stained by both LYVE-1 and Ki-67 were observed in the gastric wall of the tumor-bearing mice (Fig. 1*B*), demonstrating induction of lymphangiogenesis in this model.

Suppression of lymphangiogenesis and lymph node metastasis by etodolac in the model of lymph node metastasis. We examined whether etodolac, a COX-2 inhibitor, inhibits
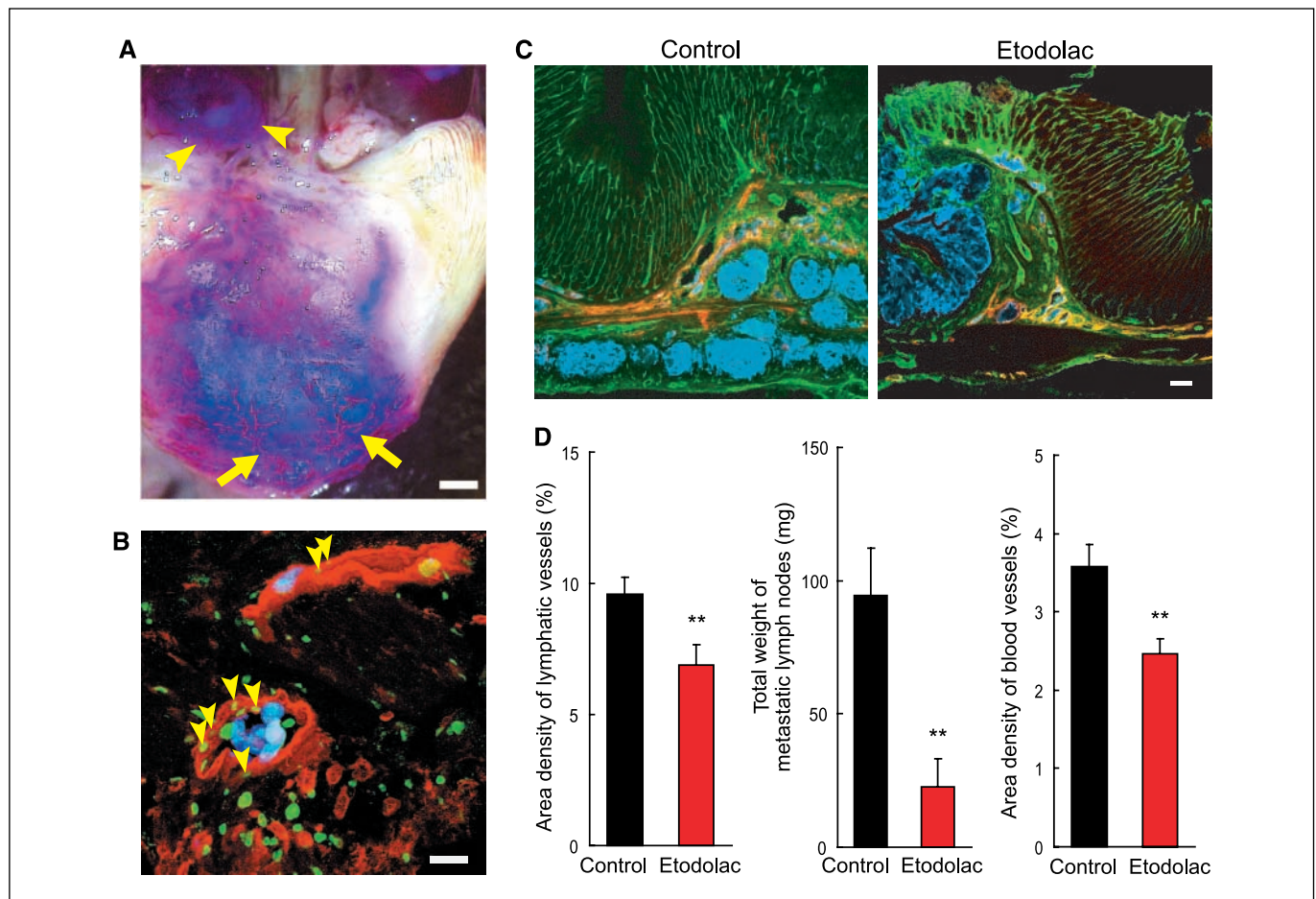
Figure 1. Effects of etodolac on a murine model of lymph node metastasis of gastric carcinoma. *A,* spread of GFP-expressing OCUM-2MLN cells 4 wk after inoculation into gastric wall of BALB/c nu/nu mouse. GFP-positive cancer cells (*purple*) which have invaded peritumoral lymphatic vessels in the gastric wall and metastasized to regional lymph nodes (*arrowheads*). *Arrows,* orthotopically inoculated OCUM-2MLN tumor. *Scale bar*, 1 mm. *B,* cross-section of gastric wall with GFP-positive cancer cells (*blue*), stained for lymphatic vessels (anti–LYVE-1; *red*) and dividing nuclei (anti–Ki-67; *green*). *Arrowheads,* lymphatic endothelial cells positive for Ki-67. *Scale bar*, 20 μm. *C,* orthotopic GFP-positive OCUM-2MLN (*blue*) tumor in control mice or in etodolac-treated mice, stained for lymphatic vessels (anti–LYVE-1; *red*) and blood vessels (anti–PECAM-1; *green*). *Scale bar*, 50 μm. *D, left,* quantification of tumor lymphatic vessels. Columns, mean area density of LYVE-1-positive pixels per microscopic field; *bars,* SE (data from one section per tumor, with 10 images per section). **, $P = 0.008$, two-sided Student's *t* test. *Middle,* total weights of metastatic lymph nodes from control mice and etodolac-treated mice. *Columns,* mean; *bars,* with SE. **, $P = 0.006$. *Right,* quantification of tumor blood vessels. *Columns,* mean area density of pixels highly positive for PECAM-1 per microscopic field; *bars,* SE. **, $P = 0.002$.
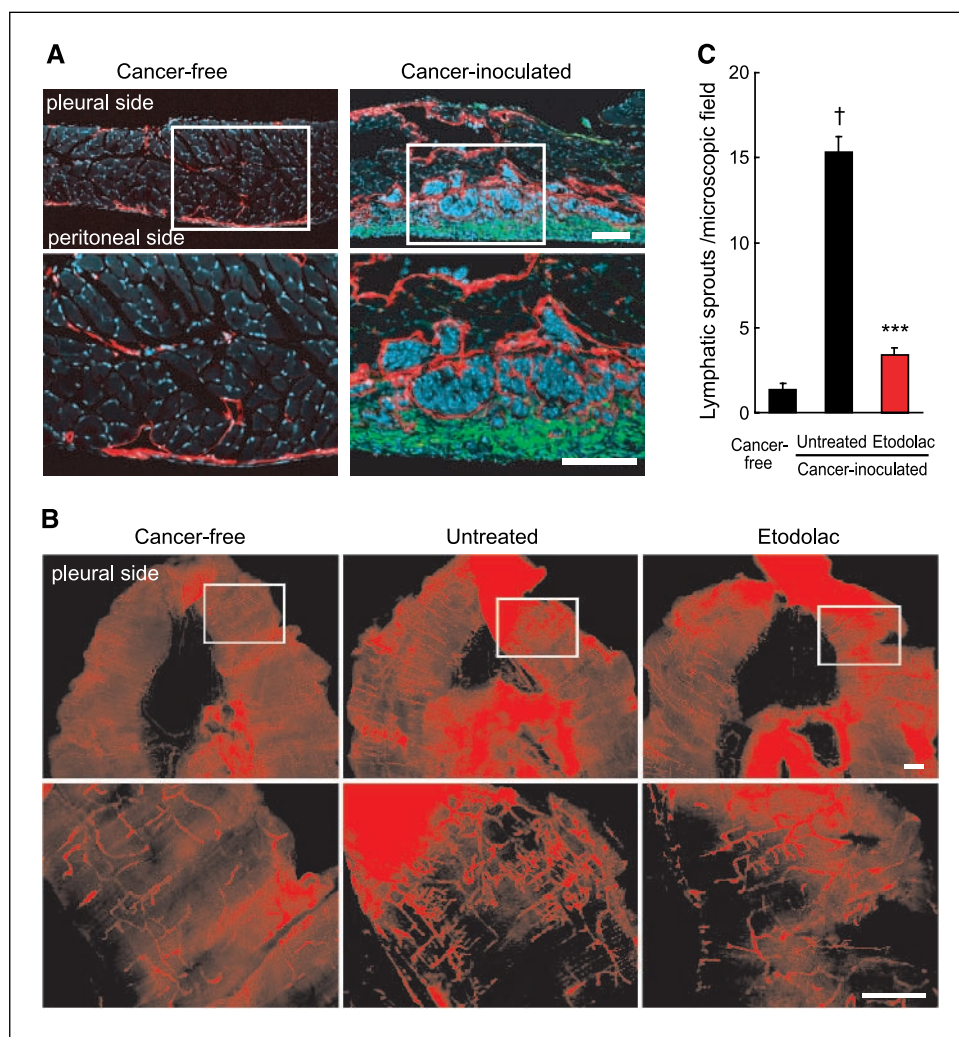
Figure 2. Effects of etodolac on lymphangiogenesis in the model of carcinomatous peritonitis. *A,* lymphatic vessels in the diaphragm in normal mice and those with carcinomatous peritonitis. Immunostaining of lymphatic vessels (anti–LYVE-1, *red*), macrophages (anti-F4/80, *green*), and nuclei (*blue*) in parasagittal sections of the diaphragm from cancer-free mice and those with carcinomatous peritonitis induced by OCUM-2MLN. *Top,* middle magnification; *bottom,* the boxed areas in the top in higher magnification. *Scale bars*, 100 μm. *B,* whole-mount immunostaining for lymphatic vessels (anti–LYVE-1, *red*) of diaphragms from cancer-free mice and those with carcinomatous peritonitis treated with vehicle control or etodolac. *Top,* images of the entire diaphragm at low power; *bottom,* the boxed areas in the top in higher magnifications. *Scale bars*, 1 mm. *C,* quantification of lymphatic sprouts. *Columns,* mean number of lymphatic sprouts per microscopic field; *bars,* SE. $n = 5$ mice for each group and 10 fields per mouse; cancer-inoculated control mice versus cancer-free mice: [†], $P < 0.001$; etodolac-treated mice versus cancer-inoculated control mice: [***], $P < 0.001$.

lymphangiogenesis and lymph node metastasis in this model. Etodolac (500 ppm in food) or vehicle control was given p.o. throughout the experimental period, from inoculation of cancer cells to evaluation of lymphangiogenesis and lymph node metastasis. We stained the sections of tumors in the gastric wall for LYVE-1. As shown in Fig. 1C, tumor lymphangiogenesis was less prominent in the etodolac-treated mice than in the control mice. Quantification of LYVE-1–positive areas in hotspots confirmed these findings (Fig. 1D, *left*). We also determined the extent of lymph node metastasis by measuring the total weight of metastatic lymph nodes identified by expression of GFP using a fluorescence stereomicroscope (Supplementary Fig. S2). Consistent with the decrease in density of lymphatic vessels, the total weight of metastatic lymph nodes was significantly less in etodolac-treated mice than in the control mice (Fig. 1D, *middle*).

To determine whether etodolac affects angiogenesis, as well as lymphangiogenesis, we examined tumor angiogenesis by staining sections of tumors for PECAM-1. The relative area occupied by vessels strongly positive for PECAM-1 was significantly decreased in the etodolac-treated mice compared with the control mice (Fig. 1D, *right*).

Lymphatic vessels in the diaphragm in normal mice and those with carcinomatous peritonitis. To evaluate tumor lymphangiogenesis in another fashion, we established a new model of lymphangiogenesis, in which the lymphatic vessels of the diaphragm of mice can be observed. We first observed the physiologic function and morphologic characteristics of lymphatic vessels in the diaphragm. Only 20 min after the injection of India ink into the abdominal cavity, lymphatic vessels in the diaphragm were stained with the ink (Supplementary Fig. S3A). Lymphatic vessels in the diaphragm were also observed by whole-mount immunostaining for LYVE-1 and Prox1 as specific markers of lymphatic vessels (Supplementary Fig. S3B). Immunostaining of sections of the diaphragm for LYVE-1 revealed a lymphatic network consisting of lymphatic lacunae on the peritoneal side and intermuscular lymphatic vessels (Fig. 2A, *left*; ref. 33).

Next, we observed the diaphragms of mice with carcinomatous peritonitis. Two weeks after i.p. inoculation of OCUM-2MLN cells (5×10^6) into BALB/c nu/nu mice, cancerous ascites had accumulated, and dissemination of cancer on the peritoneal surface of the diaphragm was observed (data not shown). Sections of diaphragm revealed that these sites of dissemination consisted of cancer cells and F4/80-positive macrophages (Fig. 2A, *right*). The lymphatic vessels in the diaphragm were increased in both size and number. Outgrowths of the lymphatic vessels into the site of dissemination were also detected (Fig. 2A).

Suppression of lymphangiogenesis by etodolac in the model of carcinomatous peritonitis. As described above, lymphatic

vessels in the diaphragm can be evaluated not only by using tissue sections but also by using whole-mount samples. Using this model, we examined the effects of etodolac on tumor lymphangiogenesis. Etodolac or vehicle control was continuously given for 2 weeks from the time of inoculation of cancer cells to evaluation of lymphangiogenesis. We observed the lymphatic vessels in the diaphragm by whole-mount immunostaining for LYVE-1 from the pleural side. More sprouts were detected along lymphatic vessels over the entire diaphragm in the cancer-inoculated mice than in the cancer-free mice (Fig. 2B). However, the number of sprouts was less in the etodolac-treated mice than in the untreated mice (Fig. 2B). Quantification of lymphatic sprouts revealed significant reduction of lymphangiogenesis by treatment with etodolac (Fig. 2C).

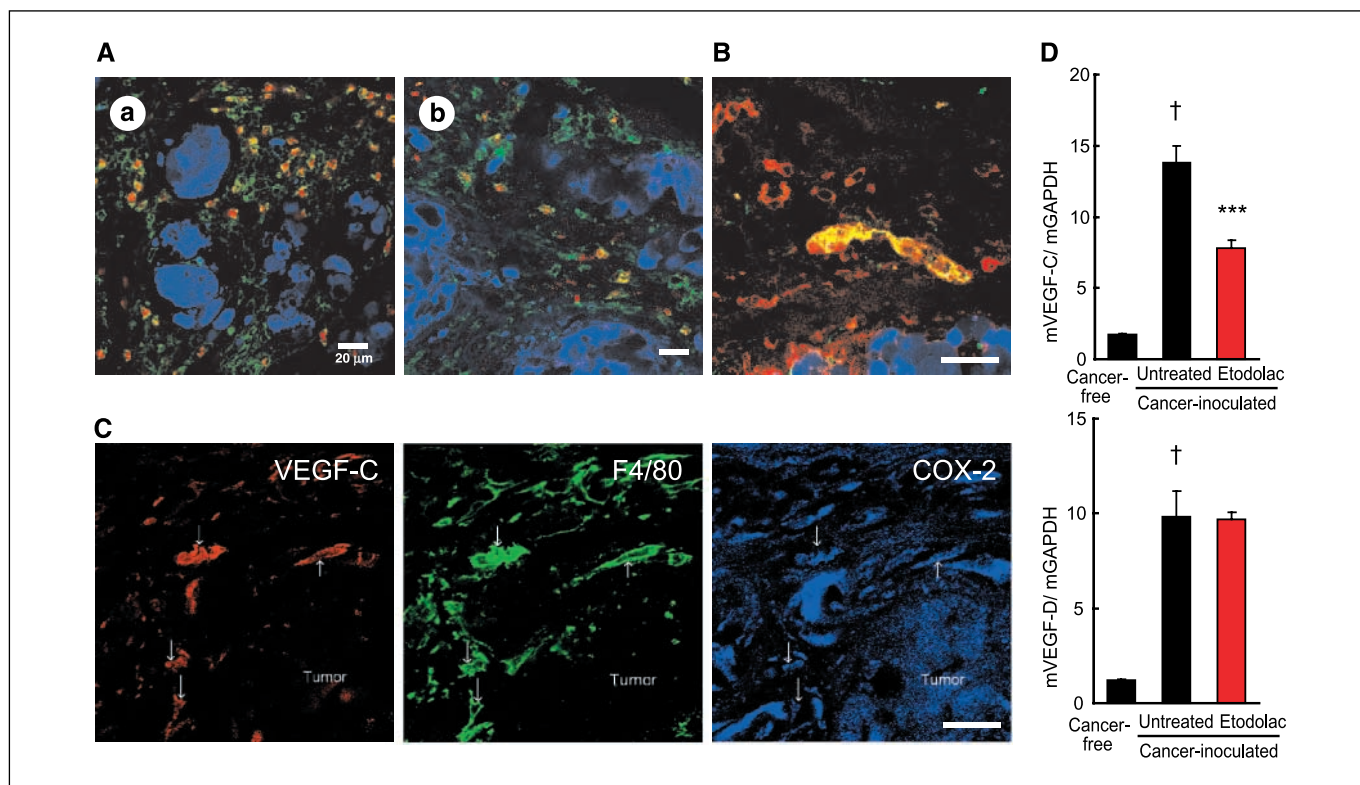**Expression of VEGF-C/VEGF-D and COX-2 in tumor tissues.** Macrophages have been suggested to be the major cellular sources of lymphangiogenic growth factors VEGF-C and VEGF-D (10–12). To determine whether macrophages are also the major source of these ligands in our model, we did immunohistochemical staining for macrophage marker F4/80 and VEGF-C or VEGF-D. In this model, many cells positive for VEGF-C (Fig. 3A, a) and VEGF-D (Fig. 3A, b) were F4/80-positive macrophages. Although certain cancer cells have also been reported to secrete these ligands, OCUM-2MLN cells were negative for VEGF-C (Fig. 3A, a) and VEGF-D (Fig. 3A, b) staining. These observations indicate that

macrophages are the major sources of lymphangiogenic growth factors in this model.

We further examined the expression of COX-2 to determine which cells are the targets of the COX-2 inhibitor etodolac. Some lymphatic endothelial cells (Fig. 3B) and OCUM-2MLN cells (Fig. 3C) expressed COX-2. As shown in Fig. 3C, some F4/80-positive macrophages were also COX-2 positive. These findings suggest that etodolac may act on several different types of cells in this model.

We also investigated the expression levels of mouse mRNA for VEGF-C (Fig. 3D, top) and VEGF-D (Fig. 3D, bottom) in the tumor tissues. Consistent with the results obtained by immunohisto-chemical analysis, mRNA level for VEGF-C and VEGF-D increased in the orthotopically inoculated tumors. In addition, the expression of VEGF-C, but not that of VEGF-D, was down-regulated after treatment with etodolac.

Effects of etodolac on macrophages, lymphatic endothelial cells, and cancer cells *in vitro*. Given the coexpression of COX-2 and VEGF-C or VEGF-D in macrophages, we hypothesized that etodolac suppresses the expression of VEGF-C and VEGF-D in macrophages. To test this hypothesis, we examined the mRNA levels of VEGF-C and VEGF-D in *in vitro*–cultured RAW264.7, a mouse macrophage-like cell line, by quantitative RT-PCR. The levels of expression of COX-2 (Fig. 4A) and VEGF-C (Fig. 4B) were dose-dependently up-regulated at 24 h after stimulation with LPS. The up-regulation of VEGF-C was, however, suppressed by

Figure 3. Expression of VEGF-C, VEGF-D, and COX-2 in tumor tissue. *A,* immunostaining of orthotopically inoculated tumors for VEGF-C (*a*) or VEGF-D (*b, red*), macrophages (anti-F4/80, *green*), and cancer cells (GFP, *blue*). Note that OCUM-2MLN cells themselves were negative for VEGF-C and VEGF-D. *Scale bar,* 20 μm. *B,* several lymphatic endothelial cells (anti–LYVE-1, *red*) in the GFP-expressing tumor (*blue*) overexpress COX-2 (*green*), suggesting that lymphatic endothelial cells in the tumor are also targets of etodolac. *Scale bar,* 20 μm. *C,* triple immunostaining for VEGF-C, F4/80, and COX-2 in the model of carcinomatous peritonitis showed colocalization of these markers. Most VEGF-C–positive cells were F4/80-positive macrophages, whereas some F4/80-positive macrophages were strongly positive for COX-2. *Arrows,* triple-positive cells. *Scale bar,* 20 μm. *D,* quantitative RT-PCR analysis of mouse mRNA for VEGF-C (*mVEGF-C, top*) and mouse mRNA for VEGF-D (*mVEGF-D*) expression (*bottom*). Both mouse mRNA for VEGF-C and VEGF-D increased in orthotopically inoculated tumors, and the expression of mouse mRNA for VEGF-C was down-regulated after 3 d of treatment with etodolac. *Columns,* mean; *bars,* SE. Cancer-inoculated control mice versus cancer-free mice: †, $P < 0.001$; etodolac-treated mice versus cancer-inoculated control mice: ***, $P < 0.001$.
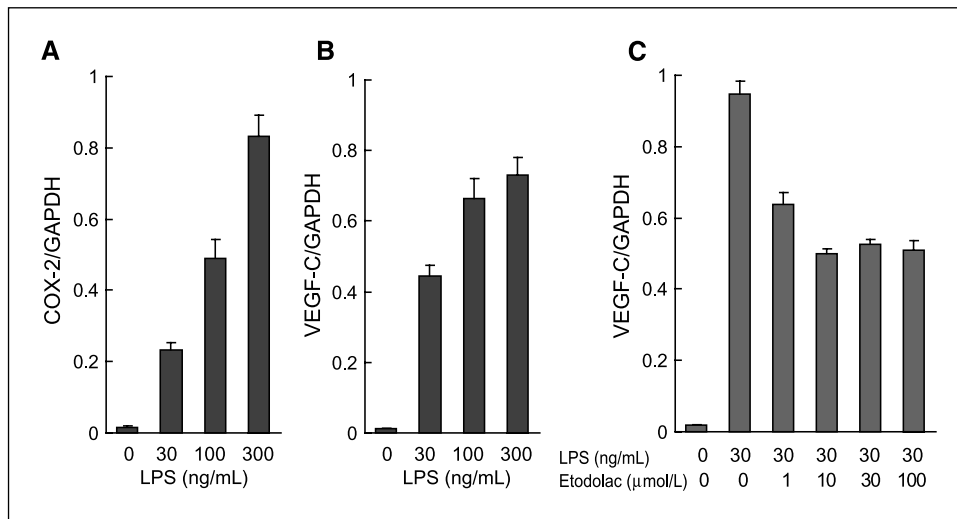
Figure 4. Suppression of expression of VEGF-C by etodolac in macrophages *in vitro*. mRNA levels of COX-2 (*A*) and VEGF-C (*B*) in cultured RAW.264.7, mouse macrophage-like cells, were determined at 24 h after stimulation with LPS. *C,* suppression of VEGF-C expression by treatment with etodolac. *Columns,* mean; *bars,* SE.

treatment with etodolac in a dose-dependent fashion. Ten micro-molars or higher concentrations of etodolac maximally, although not completely, suppressed the expression of VEGF-C mRNA (Fig. 4C). We also examined the expression of VEGF-D, but found that it was not significantly affected by etodolac (data not shown).

We further examined the effects of etodolac on cells other than macrophages which are involved in tumor lymphangiogenesis, i.e., lymphatic endothelial cells and cancer cells. We used HDLECs to investigate the effects of etodolac on lymphatic endothelial cells. The mRNA levels of VEGF-R3 in HDLECs were not affected by 10 μmol/L of etodolac (Fig. 5A). In contrast, cell growth assay revealed that 3 and 30 μmol/L of etodolac each significantly suppressed the growth of HDLECs, only upon stimulation with LPS, although the inhibitory effect of etodolac was not prominent

(Fig. 5B). We also examined the effects of etodolac on the growth of OCUM-2MLN. However, no significant difference in growth of OCUM-2MLN cells was observed at 3 days after addition of 3 or 30 μmol/L etodolac (Fig. 5C).

Suppression of lymphangiogenesis by etodolac in a mouse model of chronic inflammation. We used a mouse model of chronic inflammation to determine whether the suppressive effect of etodolac on tumor lymphangiogenesis holds true for inflammatory lymphangiogenesis. In this model, thioglycollate medium was given i.p. as a proinflammatory agent to induce chronic aseptic peritonitis. After repeated i.p. injection (thrice a week for 2 weeks) of thioglycollate medium to immunocompetent BALB/c mice, inflammatory plaques formed on the peritoneal surface of the diaphragm (Fig. 6A, *top*). These plaques were consisted mainly
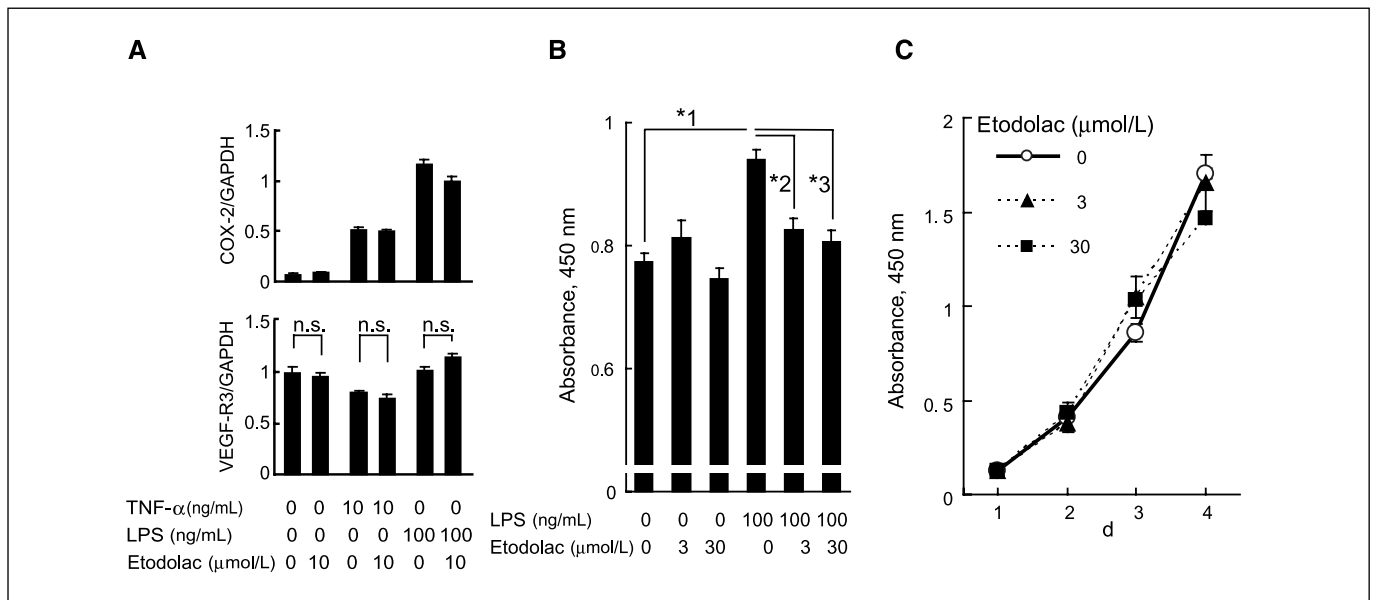
Figure 5. Effects of etodolac on cells other than macrophages. *A,* mRNA levels of VEGF-R3 (*bottom*) in HDLECs treated with 10 μmol/L of etodolac with or without stimulation with 10 ng/mL tumor necrosis factor-α (TNF-α) or 100 ng/mL LPS. *Top,* up-regulation of COX-2 in HDLECs by stimulation with TNF-α or LPS. *Columns,* mean; *bars,* SE. n.s., not significant. *B,* cell growth assay using WST-8 revealed that 3 and 30 μmol/L of etodolac each significantly suppressed the growth of HDLECs upon stimulation with 100 ng/mL LPS; *1, $P < 0.001$; *2, $P < 0.001$; *3, $P < 0.001$; Student's *t* test. *Columns,* mean; *bars,* SE. *C,* cell growth assay with WST-8 revealed that growth of OCUM-2MLN was not affected by etodolac at 3 d after addition of 3 or 30 μmol/L etodolac. *Points,* mean; *bars,* SE.

of mononuclear cells (Fig. 6*A, bottom*). Immunohistochemical analysis revealed that COX-2, VEGF-C, and VEGF-D were highly expressed in these plaques and that many cells positive for VEGF-C and VEGF-D were F4/80-positive macrophages (Fig. 6*B*).

Using this model, we examined whether etodolac inhibits inflammatory lymphangiogenesis. As shown in Fig. 6*C*, outgrowths of lymphatic vessels in the plaques were decreased in etodolac-treated mice compared with untreated mice. Quantification of LYVE-1–positive areas in the plaques revealed that induction of lymphangiogenesis was significantly suppressed in etodolac-treated mice compared with control mice (Fig. 6*D*). These findings indicate that etodolac is able to suppress lymphangiogenesis in tumor tissues, as well as in nontumorous tissue.

Discussion

Many clinical and animal studies have shown that COX-2 induces angiogenesis (34). Meanwhile, there is no direct evidence of a relationship between COX-2 and lymphangiogenesis, although some clinical and animal studies have suggested that level of COX-2 expression in tumor tissue is correlated with lymph node metastasis and/or unfavorable prognosis (24–28, 35). However, none of these studies clearly indicated the status of lymphatic vessels. In the present study, we investigated the effects of COX-2 inhibitor on lymphatic vessels using the lymphatic endothelial cell-specific markers LYVE-1 and Prox1. In the model of lymphatic metastasis, both lymphangiogenesis and angiogenesis were induced around the orthotopic tumors of OCUM-2MLN. We found

Figure 6. Effects of etodolac on lymphangiogenesis in mouse model of chronic aseptic peritonitis. *A, top,* macroscopic appearance of the diaphragm of BALB/c mouse after repeated i.p. injection (thrice a week for 2 wk) of thioglycollate medium. Inflammatory plaques formed on the peritoneal surface of the diaphragm (*arrows*). *Scale bar,* 5 mm. *Bottom,* H&E staining of cross-section of inflammatory plaques on diaphragm. *Scale bar,* 50 μm. *Inset,* enlargement of the boxed area. *B,* immunohistochemical staining of COX-2 (*a and d*), VEGF-C (*b and e*), and VEGF-D (*c and f*) in plaques on diaphragms. Each antibody was displayed in the red channel. *d–f,* double-staining with each antibody and anti-F4/80 (*green*). Nuclear counterstaining was done with TOTO-3 (*blue*). *Scale bars,* 50 μm (*a–c*) and 10 μm (*d–f*). *C,* immunostaining of the inflammatory plaques on diaphragm from control or etodolac-treated mice (*n* = 5 for each group). *Top,* whole-mount staining with the lymphatic vessel marker (anti–LYVE-1, *red*); *middle,* merged images stained also with macrophage marker (anti-CD11b, *green*); *bottom,* cross-sections stained for F4/80 (*green*) and LYVE-1 (*red*). *Scale bar,* 50 μm. *D,* quantification of lymphatic vessels in plaques. *Columns,* mean area densities of LYVE-1–positive pixels per microscopic field; *bars,* SE (10 fields per mouse); ***, *P* < 0.001.
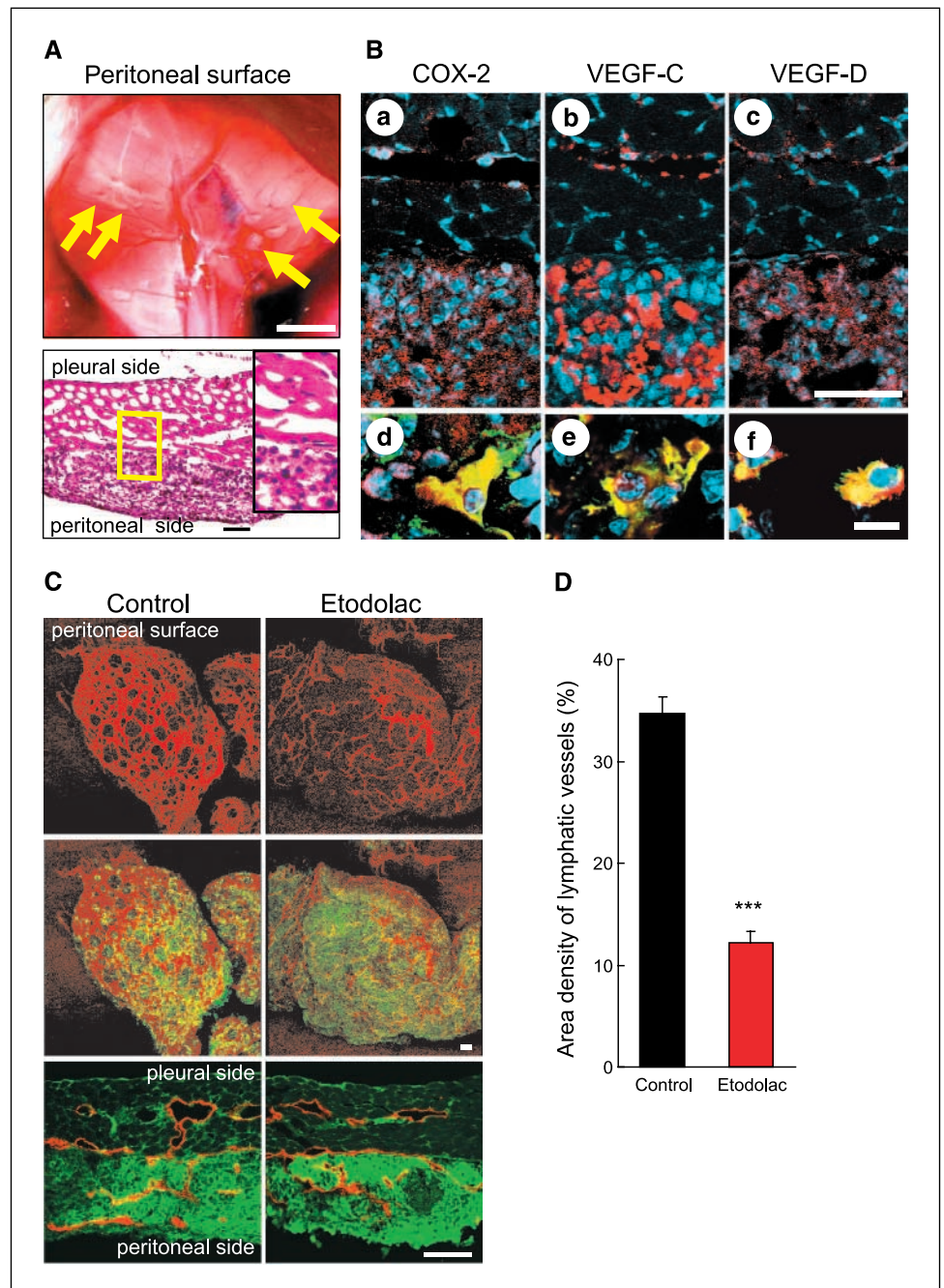
that administration of etodolac suppressed tumor lymphangiogenesis along with tumor angiogenesis. In addition, we evaluated the extent of lymph node metastasis and found that the total weight of metastasized lymph nodes was also decreased by treatment with etodolac. These findings indicated that COX-2 promotes tumor lymphangiogenesis and consequent lymph node metastasis, in addition to tumor angiogenesis as previously reported.

The reproducibility of assignment of highly vascularized areas, i.e., hotspots in tumor tissue sections, is a critical variable in the analysis of lymphangiogenesis (36). Finding relevant hotspots requires training and experience (37). To deal with this potential problem, we established here a new model of tumor lymphangiogenesis in the diaphragm. Since lymphatic vessels in the diaphragm can be immunostained in whole-mount preparations, it is possible to capture the entire network of lymphatics in the diaphragm. There is no need to pick only hotspots for quantification because outgrowth of lymphatic vessels was observed over the entire diaphragm in the model of carcinomatous peritonitis. We quantified the number of sprouts of lymphatic vessels as a marker of lymphangiogenesis, as suggested by Baluk et al. (11). The results using this model confirmed the finding that etodolac suppresses lymphangiogenesis.

Recent studies have shown that inflammatory cells have stimulatory effects on tumor progression (38). In particular, tumor-associated macrophages have been suggested to promote tumor lymphangiogenesis (10, 39). We therefore hypothesized that etodolac suppresses the secretion of lymphangiogenic factors from macrophages. Our finding that some macrophages in tumor stroma expressed COX-2 strongly supports this hypothesis. Furthermore, we found that mRNA levels of VEGF-C was indeed suppressed by etodolac in RAW264.7 cells, as well as in tumor tissues *in vivo*. Although these findings are not in agreement with a previous report that VEGF-C expression in fibroblasts was not suppressed by indomethacin, a nonselective NSAID (40), this discrepancy may be due to the difference in cell types examined or the COX-2 selectivity of drugs used.

Lymphangiogenesis is also induced in chronic inflammatory lesions (41). Macrophages have recently been shown to be recruited into inflammatory lesions to secrete VEGF-C and induce lymphangiogenesis (11, 12). In the present study, using a model of chronic aseptic peritonitis, we observed that macrophages densely accumulated in inflammatory plaques, wherein lymphangiogenic growth factors are expressed. These findings suggest that COX-2 can enhance lymphangiogenesis in the absence of cancer cells.

We have shown that decrease of lymph node metastasis can be achieved by COX-2 inhibitor, possibly via inhibition of macrophage-mediated lymphangiogenesis. Despite recent studies reporting cardiovascular complications from long-term administration of NSAIDs (42), these drugs may still be applicable to cancer treatment by limiting population and administrating periods: NSAIDs should be effective for preventing potential metastases in patients with advanced cancers in presurgical period or in those having inflammation aroused by surgical manipulation in early postsurgical periods. In the latter case, surgery-related inflammation may be accompanied by lymphangiogenesis, which can be a cause of dissemination or metastasis of unexpectedly remained cancer cells.

In conclusion, we believe that our findings may provide a potential usage of COX-2 inhibitors in cancer treatment, which could overcome known obstacles in using these drugs.

Acknowledgments

References

1. Alitalo K, Tammela T, Petrova TV. Lymphangiogenesis in development and human disease. Nature 2005;438: 946–53.
2. Achen MG, Stacker SA. Tumor lymphangiogenesis and metastatic spread-new players begin to emerge. Int J Cancer 2006;119:1755–60.
3. Pepper MS. Lymphangiogenesis and tumor metastasis: myth or reality? Clin Cancer Res 2001;7:462–8.
4. Pepper MS, Tille JC, Nisato R, Skobe M. Lymphangiogenesis and tumor metastasis. Cell Tissue Res 2003;314: 167–77.
5. Nakamura Y, Yasuoka H, Tsujimoto M, et al. Importance of lymph vessels in gastric cancer: a prognostic indicator in general and a predictor for lymph node metastasis in early stage cancer. J Clin Pathol 2006;59: 77–82.
6. Achen MG, McColl BK, Stacker SA. Focus on lymphangiogenesis in tumor metastasis. Cancer Cell 2005;7:121–7.
7. Shimizu K, Kubo H, Yamaguchi K, et al. Suppression of VEGFR-3 signaling inhibits lymph node metastasis in gastric cancer. Cancer Sci 2004;95: 328–33.
8. Yonemura Y, Endo Y, Fujita H, et al. Role of vascular endothelial growth factor C expression in the development of lymph node metastasis in gastric cancer. Clin Cancer Res 1999;5:1823–9.
9. Kitadai Y, Kodama M, Cho S, et al. Quantitative analysis of lymphangiogenic markers for predicting metastasis of human gastric carcinoma to lymph nodes. Int J Cancer 2005;115:388–92.
10. Schoppmann SF, Birner P, Stockl J, et al. Tumor-associated macrophages express lymphatic endothelial growth factors and are related to peritumoral lymphangiogenesis. Am J Pathol 2002;161:947–56.
11. Baluk P, Tammela T, Ator E, et al. Pathogenesis of persistent lymphatic vessel hyperplasia in chronic airway inflammation. J Clin Invest 2005;115:247–57.
12. Cursiefen C, Chen L, Borges LP, et al. VEGF-A stimulates lymphangiogenesis and hemangiogenesis in inflammatory neovascularization via macrophage recruitment. J Clin Invest 2004;113:1040–50.
13. Thun MJ, Henley SJ, Patrono C. Nonsteroidal anti-inflammatory drugs as anticancer agents: mechanistic, pharmacologic, and clinical issues. J Natl Cancer Inst 2002;94:252–66.
14. Dannenberg AJ, Altorki NK, Boyle JO, et al. Cyclooxygenase 2: a pharmacological target for the prevention of cancer. Lancet Oncol 2001;2:544–51.
15. Ristimaki A, Honkanen N, Jankala H, Sipponen P, Harkonen M. Expression of cyclooxygenase-2 in human gastric carcinoma. Cancer Res 1997;57:1276–80.
16. Saukkonen K, Nieminen O, van Rees B, et al. Expression of cyclooxygenase-2 in dysplasia of the stomach and in intestinal-type gastric adenocarcinoma. Clin Cancer Res 2001;7:1923–31.
17. Oshima M, Dinchuk JE, Kargman SL, et al. Suppression of intestinal polyposis in Apc$^{\Delta 716}$ knockout mice by inhibition of cyclooxygenase 2 (COX-2). Cell 1996;87: 803–9.
18. Kawamori T, Rao CV, Seibert K, Reddy BS. Chemopreventive activity of celecoxib, a specific cyclooxygenase-2 inhibitor, against colon carcinogenesis. Cancer Res 1998;58:409–12.
19. Wang D, Mann JR, DuBois RN. The role of prostaglandins and other eicosanoids in the gastrointestinal tract. Gastroenterology 2005;128:1445–61.
20. Tsujii M, Kawano S, Tsuji S, Sawaoka H, Hori M, DuBois RN. Cyclooxygenase regulates angiogenesis induced by colon cancer cells. Cell 1998;93:705–16.
21. Williams CS, Tsujii M, Reese J, Dey SK, DuBois RN. Host cyclooxygenase-2 modulates carcinoma growth. J Clin Invest 2000;105:1589–94.
22. Leahy KM, Ornberg RL, Wang Y, Zweifel BS, Koki AT, Masferrer JL. Cyclooxygenase-2 inhibition by celecoxib reduces proliferation and induces apoptosis in angiogenic endothelial cells *in vivo*. Cancer Res 2002; 62:625–31.
23. Masferrer JL, Leahy KM, Koki AT, et al. Antiangiogenic and antitumor activities of cyclooxygenase-2 inhibitors. Cancer Res 2000;60:1306–11.
24. Su JL, Shih JY, Yen ML, et al. Cyclooxygenase-2 induces EP1- and HER-2/Neu-dependent vascular endothelial growth factor-C up-regulation: a novel mechanism of lymphangiogenesis in lung adenocarcinoma. Cancer Res 2004;64:554–64.
25. Timoshenko AV, Chakraborty C, Wagner GF, Lala PK. COX-2-mediated stimulation of the lymphangiogenic factor VEGF-C in human breast cancer. Br J Cancer 2006;94:1154–63.
26. Siironen P, Ristimaki A, Narko K, et al. VEGF-C and

COX-2 expression in papillary thyroid cancer. Endocr Relat Cancer 2006;13:465–73.

27. Soumaoro LT, Uetake H, Takagi Y, et al. Coexpression of VEGF-C and Cox-2 in human colorectal cancer and its association with lymph node metastasis. Dis Colon Rectum 2006;49:392–8.

28. Zhang J, Ji J, Yuan F, et al. Cyclooxygenase-2 expression is associated with VEGF-C and lymph node metastases in gastric cancer patients. Biomed Pharmacother 2005;59 [Suppl]:S285–8.

29. Glaser K, Sung ML, O'Neill K, et al. Etodolac selectively inhibits human prostaglandin G/H synthase 2 (PGHS-2) versus human PGHS-1. Eur J Pharmacol 1995;281:107–11.

30. Warner TD, Giuliano F, Vojnovic I, Bukasa A, Mitchell JA, Vane JR. Nonsteroid drug selectivities for cyclo-oxygenase-1 rather than cyclo-oxygenase-2 are associated with human gastrointestinal toxicity: a full *in vitro* analysis. Proc Natl Acad Sci U S A 1999;96:7563–8.

31. Fujihara T, Sawada T, Hirakawa K, et al. Establishment of lymph node metastatic model for human gastric cancer in nude mice and analysis of factors associated with metastasis. Clin Exp Metastasis 1998;16:389–98.

32. Shibuya K, Shirakawa J, Kameyama T, et al. CD226 (DNAM-1) is involved in lymphocyte function-associated antigen 1 costimulatory signal for naive T cell differentiation and proliferation. J Exp Med 2003;198:1829–39.

33. Abu-Hijleh MF, Habbal OA, Moqattash ST. The role of the diaphragm in lymphatic absorption from the peritoneal cavity. J Anat 1995;186:453–67.

34. Iniguez MA, Rodriguez A, Volpert OV, Fresno M, Redondo JM. Cyclooxygenase-2: a therapeutic target in angiogenesis. Trends Mol Med 2003;9:73–8.

35. Tendo M, Yashiro M, Nakazawa K, et al. Inhibitory effect of a selective cyclooxygenase inhibitor on the invasion-stimulating activity of orthotopic fibroblasts for scirrhous gastric cancer cells. Cancer Sci 2005;96:451–5.

36. Van der Auwera I, Cao Y, Tille JC, et al. First international consensus on the methodology of lymphangiogenesis quantification in solid human tumours. Br J Cancer 2006;95:1611–25.

37. Vermeulen PB, Gasparini G, Fox SB, et al. Second international consensus on the methodology and criteria of evaluation of angiogenesis quantification in solid human tumours. Eur J Cancer 2002;38:1564–79.

38. Coussens LM, Werb Z. Inflammation and cancer. Nature 2002;420:860–7.

39. Dadras SS, Paul T, Bertoncini J, et al. Tumor lymphangiogenesis: a novel prognostic indicator for cutaneous melanoma metastasis and survival. Am J Pathol 2003;162:1951–60.

40. Ristimaki A, Narko K, Enholm B, Joukov V, Alitalo K. Proinflammatory cytokines regulate expression of the lymphatic endothelial mitogen vascular endothelial growth factor-C. J Biol Chem 1998;273:8413–8.

41. Pullinger BD, Florey HW. Proliferation of lymphatics in inflammation. J Pathol Bact 1937;45:157–70.

42. Antman EM, Bennett JS, Daugherty A, Furberg C, Roberts H, Taubert KA. Use of nonsteroidal antiinflammatory drugs: an update for clinicians: a scientific statement from the American Heart Association. Circulation 2007;115:1634–42.

AACR American Association for Cancer Research

Inhibition of Cyclooxygenase-2 Suppresses Lymph Node Metastasis via Reduction of Lymphangiogenesis

Caname Iwata, Mitsunobu R. Kano, Akiyoshi Komuro, et al.

Updated version	Access the most recent version of this article at: http://cancerres.aacrjournals.org/content/67/21/10181
Supplementary Material	Access the most recent supplemental material at: http://cancerres.aacrjournals.org/content/suppl/2007/10/30/67.21.10181.DC1

Cited articles	This article cites 42 articles, 15 of which you can access for free at: http://cancerres.aacrjournals.org/content/67/21/10181.full.html#ref-list-1
Citing articles	This article has been cited by 19 HighWire-hosted articles. Access the articles at: /content/67/21/10181.full.html#related-urls

E-mail alerts	Sign up to receive free email-alerts related to this article or journal.
Reprints and Subscriptions	To order reprints of this article or to subscribe to the journal, contact the AACR Publications Department at pubs@aacr.org.
Permissions	To request permission to re-use all or part of this article, contact the AACR Publications Department at permissions@aacr.org.